JOURNAL OF GEOPHYSICAL RESEARCH, VOL. 113, A03302, doi:10.1029/2007JA012335, 2008

Investigation of the response of equatorial MLTI region during a partial solar eclipse through ground-based daytime optical technique

C. Vineeth,[1] Tarun K. Pant,[1] Smitha V. Thampi,[1] R. Sridharan,[1] Sudha Ravindran,[1] C. V. Devasia,[1] K. Kishore Kumar,[1] and S. Alex[2]

Received 9 February 2007; revised 14 September 2007; accepted 20 November 2007; published 11 March 2008.

[1] First experimental evidence for solar eclipse induced changes in the equatorial mesopause and the thermosphere ionosphere regions using daytime optical photometer is presented. The photometer was operated in scanning mode to probe the thermosphere and mesopause regions simultaneously in North-South direction over Trivandrum (8.5°N; 77°E; dip lat. 0.5°N) during a partial solar eclipse event on 03 October 2005. This provided a unique data set of thermosphere and mesopause regions over a horizontal distance of 600 and 240 km respectively from zenith during this event. The striking feature observed during the eclipse is the enhancement in the thermospheric O(^{1}D) 630 nm dayglow intensity and its equatorward movement. Another noteworthy observation is an overall enhancement in the mesopause temperature, more pronounced (~25–30 K) over zenith. These observations are discussed in context of the vertical coupling of the mesopause with thermosphere-ionosphere region.

Citation: Vineeth, C., T. K. Pant, S. V. Thampi, R. Sridharan, S. Ravindran, C. V. Devasia, K. Kishore Kumar, and S. Alex (2008), Investigation of the response of equatorial MLTI region during a partial solar eclipse through ground-based daytime optical technique, *J. Geophys. Res.*, *113*, A03302, doi:10.1029/2007JA012335.

1. Introduction

[2] Many experimental and modeling studies in the recent past have clearly highlighted the importance and need to investigate the mesopause, lower thermosphere and ionosphere (MLTI) region and the coupling processes involved therein and, that our comprehension regarding them is still far from complete. Recent international programs like PSMOS (Planetary Scale Mesopause Observing System) and CAWSES (Climate And Weather of the Sun-Earth System) have brought out some new results concerning these aspects of MLTI. Nevertheless, it is understood today that the mesopause energetics and dynamics over equatorial latitudes is governed to a significant extent by large and small scale dynamical features such as tides and waves present locally and by those generated elsewhere in the atmosphere below. On the other hand the daytime variability in the low latitude *F* region ionospheric density is primarily electro-dynamically controlled [*Sastri et al.*, 2003, and references therein]. In general, all the aspects of MLTI that deal with the changes in its energetic and dynamics through the wave and tidal forcing have been studied extensively across the globe. However, the response of MLTI as a whole to the sudden changes in the direct solar radiation is not well understood. In this context, the occurrence of a solar eclipse provides a unique opportunity to investigate the effects of the fast varying solar flux not only on the electrodynamics and photochemistry of the equatorial ionosphere but also on the mesopause energetics and dynamics.

[3] In the past, significant eclipse induced effects have been observed in the ionosphere and discussed [*Altadill et al.*, 2001, and references therein; *Sridharan et al.*, 2002]. In the mesosphere in altitude range of 50–65 km, the eclipse effects have been observed to be manifesting as a lowering in temperature by as much as ~3–5°K and zonal wind speed by ~6 m/s during a partial solar eclipse [*Randhawa*, 1974]. Prominent gravity wave-like structures in the ionosphere with periodicities varying from one to few hours after the maximum of solar occultation by the moon and at distances away from eclipse totality have also been reported from mid latitudes [*Altadill et al.*, 2001; *Farges et al.*, 2001]. In a detailed study conducted during the 11 August 1999 solar eclipse from Indian longitudes, it was shown that the equatorial electrodynamics underwent significant changes as a result of a pre dusk eclipse-induced ionospheric and thermospheric processes operating with their characteristic time-scales. The main ionospheric changes observed were (i) the sudden intensification of a weak blanketing Es layer (ii) significant increase in h'F immediately following the eclipse and (iii) distinctly different spatial and temporal structures in the spread-F irregularity drift velocities [*Sridharan et al.*, 2002]. No major changes were observed in the *F* region ionospheric density. In the past, the electron densities in the D and E regions of the ionosphere have been found to decrease rapidly with the onset of the eclipse [*Kane*, 1966]. The ionospheric measurements during the solar eclipse of 16 February 1980 from India reveal that the ionospheric response time is different at

[1] Space Physics Laboratory, Vikram Sarabhai Space Centre, Trivandrum, India.
[2] Indian Institute of Geomagnetism, Navi Mumbai, India.

0148-0227/08/2007JA012335$09.00

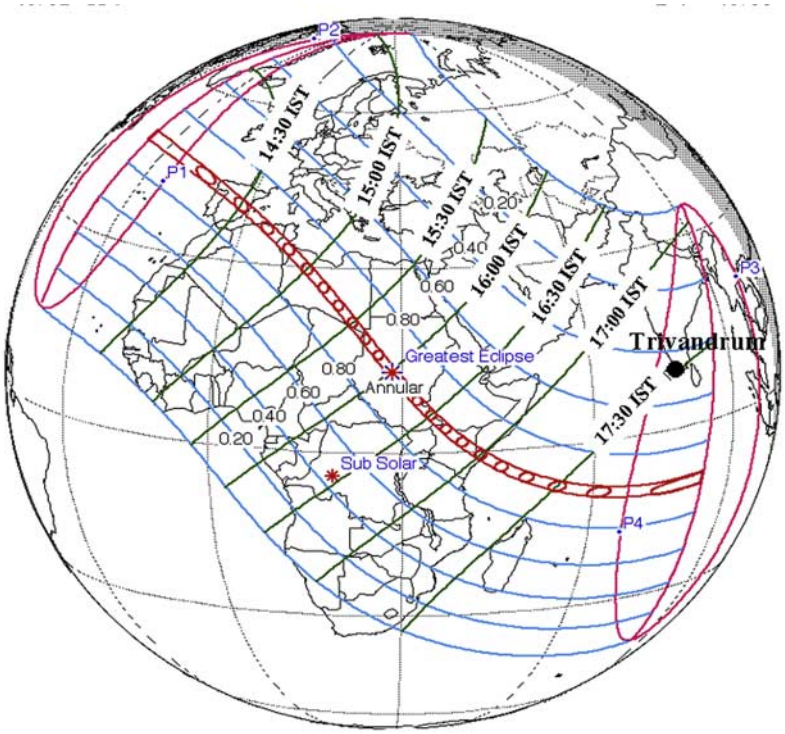

Figure 1. Path of the annular solar eclipse of 03 October 2005 over the globe (*Courtesy: Fred Espanak, NASA/GSFC* (/Sun earth.gsfc.nasa.gov/eclipse/eclipse.html)). The red line with small circle represents the path of totality. Blue lines denote the regions experiencing partial eclipse. The percentage obscuration is also mentioned on these lines. The green lines represent the progression of eclipse in Indian Standard Time.

different heights [*Balan et al.*, 1982]. Globally, both increase and decrease in F-region electron density have been reported during a solar eclipse [*Evans*, 1965]. In the American longitudes, *Ledig et al.* [1946] while discussing the ionospheric measurements from Huancayo, Peru also reported an increase in the F-region electron density, followed by a decrease, during a solar eclipse. In a more recent study, while discussing the ionospheric response to total solar eclipse over Arecibo, it has been shown that the top and bottomside ionospheres respond differently to the eclipse. It was shown that the topside ionosphere is characterized by a downward motion arising from contraction of the plasma while N_mF_2 lowered only by 50% [*Macpherson et al.*, 2000]. However, the eclipse effects in the mesopause altitudes (~85–90 km) have not yet been well explored primarily due to the lack of suitable experimental technique to probe this region.

[4] In recent years, ground-based spectrometry of specific atmospheric emissions during both day and nighttime, has enabled the simultaneous measurement/estimation of key parameters representing the mesopause (e.g., the mesopause temperature), and higher above [e.g., *Meriwether*, 1985; *Takahashi et al.*, 1998; *Sridharan et al.*, 1999; *Taylor et al.*, 2001; *Vineeth et al.*, 2005]. In this context, the unique dayglow photometers developed in India had been successfully making not only the daytime mesopause temperature measurements but also the thermospheric O^1D 630 nm dayglow intensity, almost simultaneously over Indian longitudes in recent years. These daytime atmospheric airglow intensity measurements from India, have led to some new insight into the dynamics of the mesopause, thermosphere and ionosphere over low and equatorial latitudes [*Sridharan et al.*, 1994; *Pant et al.*, 2004; *Vineeth et al.*, 2005]. The central objective of the present study is to report the simultaneous observations of the mesopause temperature and thermospheric $O(^1D)$ 630 nm airglow emissions over Trivandrum (8.5°N; 77°E; dip lat. 0.5°N) using a dayglow photometer during an annular solar eclipse event. The significance of the present study lies in showing the observational evidence for the response of MLTI region even for transient changes in solar forcing.

2. Experimental Techniques

[5] The daytime airglow intensity measurements were made using Multi Wavelength Dayglow PhotoMeter (MWDPM) on two rotational lines at 731.6 and 740.2 nm in the OH Meinel (8-3) band and at $O(^1D)$ 630.0 nm at Trivandrum. These daytime measurements were made between 0800 and the sunset, i.e., 1830 h and at various elevations between ±20° scanning from north to south along the meridian. The maximum horizontal distance covered for thermospheric measurements is ~±600 km (~6° latitude) about the dip equator, assuming $O(^1D)$ 630.0 nm emission peak to be around ~220 km. Mesopause observations cover ±240 km, assuming OH emissions peak at around ~87 km in altitude. The daytime OH emission intensity measurements at the wavelengths mentioned above were used to

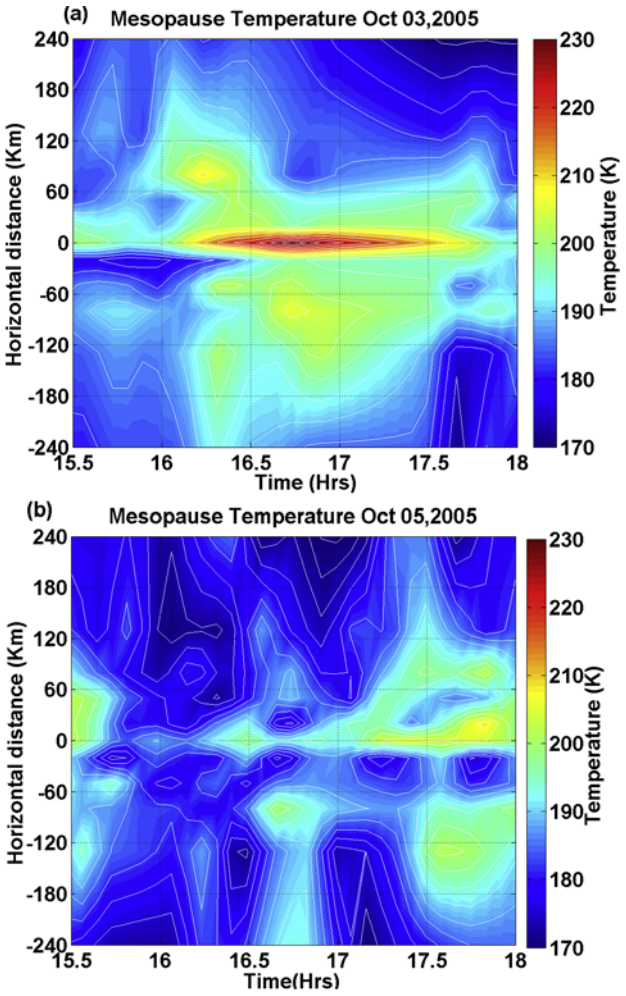

Figure 2. (a and b). Shows the spatiotemporal variations (contour lines are also shown) of the optically estimated mesopause temperature along the meridian at various elevations on 03 October 2005 (eclipse day) and 05 October 2005 (control day) respectively. Positive and negative signs on the *Y* axis represent the northern and southern directions with respect to the zenith. *X* axis represents the Indian Standard Time (IST).

estimate the daytime mesopause temperature [*Krassovsky*, 1972]. The mesopause temperature estimated using day-glow emission intensities measured by this MWDPM has already been compared and validated with the in situ WINDII satellite measured temperature and also with a collocated meteor wind radar measured temperature in the Indian region [*Vineeth et al.*, 2005].

[6] To complement the present observations with ionospheric measurements, the total electron content (TEC) data from a collocated coherent radio beacon receiver and a Global Positioning System (GPS) receiver are analyzed. This coherent radio beacon receiver receives the phase coherent 150 and 400 MHz transmissions from Low-Earth Orbiting (LEO) Navy Ionospheric Monitoring System (NIMS), USA, satellites and measures the differential Doppler between them, which is proportional to the line of sight or slant TEC (STEC). These STECs are converted to vertical TEC (VTEC) considering the angle between the raypath and the vertical at the Ionospheric Pierce Point (IPP) altitude. The IPP is taken as 300 km in the present study. It may be noted that the IPP height is usually estimated based on the height of the altitude of the maximum electron density of the ionosphere [*Birch et al.*, 2002 and the references therein]. In case of the GPS receiver, the ionosphere introduces a time delay in the 1.57542 GHz (L1) and 1.22760 GHz (L2) simultaneous transmissions from GPS satellites orbiting at ~20,000 km. The relative Ionospheric delay of the two signals is proportional to the total number of electrons along the raypath or the total electron content (TEC) [*Ho et al.*, 1996].

3. Observations

[7] The solar eclipse event of 03 October 2005 occurred over Indian longitudes during evening hours. Over Trivandrum, only partial solar eclipse was observed with ~39% obscuration, gradually decreasing with latitude to ~3.5% at Delhi (28°N, 77°E). The eclipse event over Trivandrum lasted for about two hours up to ~19:00 IST (Indian Standard Time, i.e., IST = Universal Time+5:30 min), the time of first contact being at 16:20 IST and maximum at 17:30 IST. The equatorial and low latitude regions in India went under the moon's shadow almost simultaneously. The path of the eclipse totality (red line) is shown in Figure 1. The numbers written on green line are the time in IST and the numbers on blue line represents the percentage of obscuration. The location of Trivandrum is marked as black dot on the map.

[8] Figures 2a and 2b show the spatiotemporal variations (contour lines are also shown) of the optically estimated mesopause temperature along the meridian at various elevations on 03 and 05 October 2005 respectively. Positive and negative signs on the *Y* axis represent the northern and southern directions with respect to the zenith. 05 October 2005,a nearby day (Figure 2b) is taken as the control day. On the day of the eclipse (Figure 2a), the temperature at northern locations shows an enhancement around 16:20 IST. However, within a narrow region (~30–40 km) around zenith the enhancement is more and is as high as ~25 K at 16:50 IST. The maximum enhancement in the temperature in southern direction occurs ~30 m later than that over northern direction. The temperature enhancement along the meridian exhibits a wavelike oscillation in the south-east direction with a wavelength of ~100-120 km. It must be mentioned that no such enhancement is observed in the mesopause temperature on the control day. However, on the control day, the presence of small wavelike modulations aligned to the meridian around the local sunset, i.e., 17:30–18:00 IST is seen. The temperature over zenith also shows an increase (~5-10 K) during this period.

[9] In another representation, Figures 3a and 3b shows the time history of the variations at every 15-min interval in the mesopause temperature along the meridian for the eclipse and control days. The mean temperature trends (best fits) are also depicted in each panel (dotted line). The temperature on the control day exhibits the presence of small-scale (~50–100 km) modulations with almost uniform mean temperature. The mean temperatures (dotted lines) before 16:15 IST are almost same (~185 K) for the

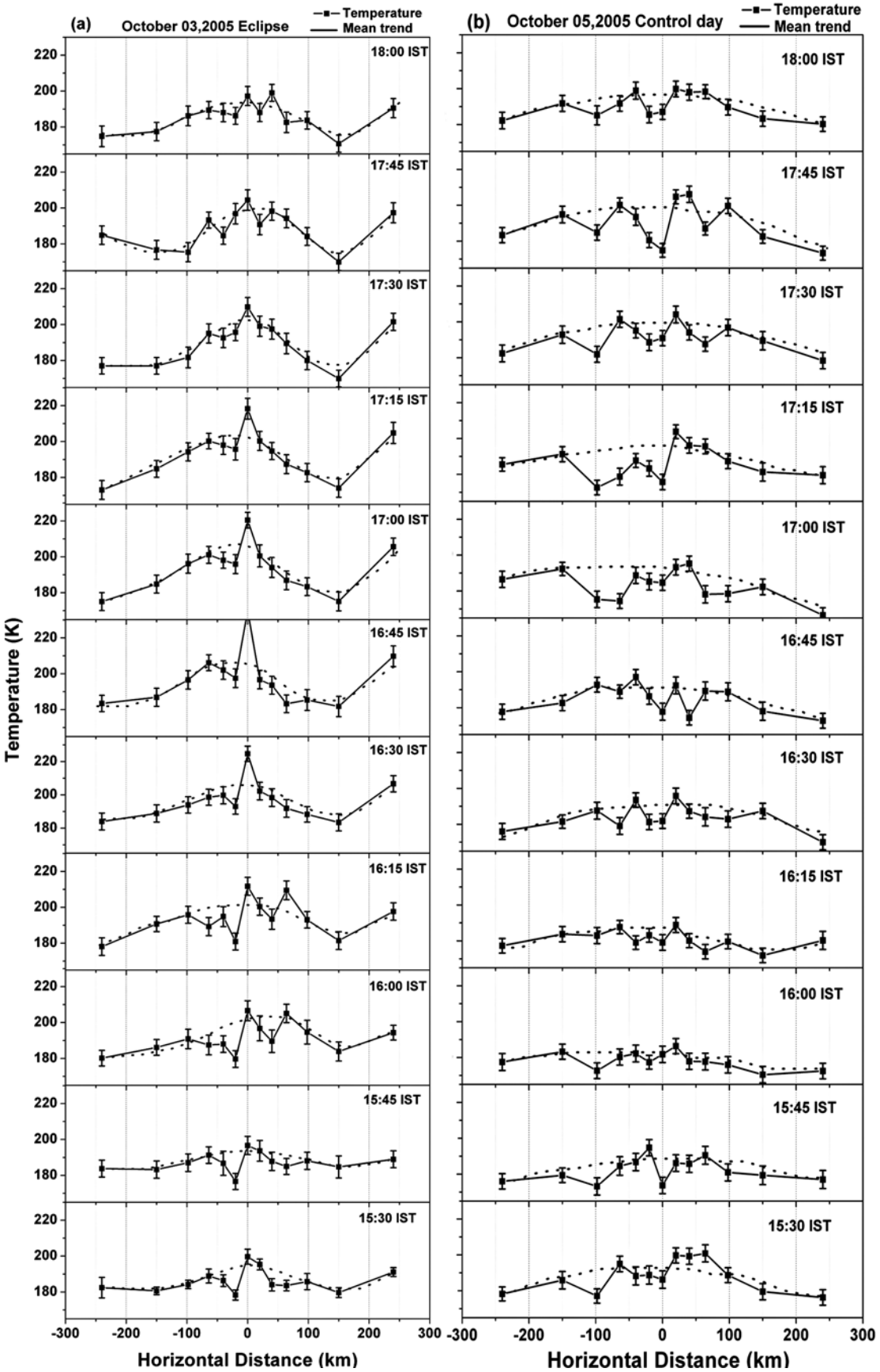

Figure 3. (a and b). Exhibits the time history of the variations at every 15 m interval in the mesopause temperature along the meridian for the 03 October 2005 (eclipse day) and 05 October 2005 (control day).

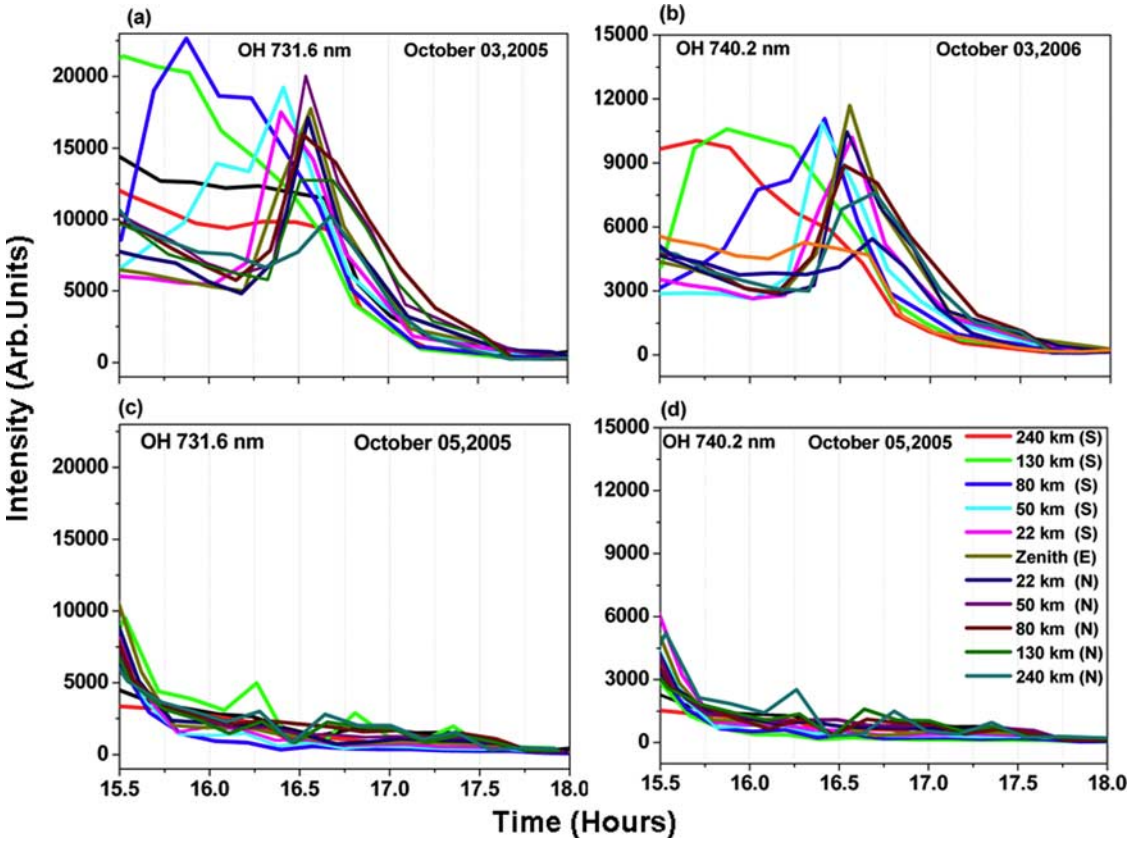

Figure 4. The temporal variation of OH airglow intensities (arbitrary units) 731.6 nm and 740.2 nm respectively at various elevation on the eclipse day (a and b) and control day (c and d).

eclipse and the control day. It rises at 16:45 IST to ~210 K from ~185 K at 15:30 IST. As discussed earlier, a prominent enhancement in temperature in the region ±50 km around zenith is quite conspicuous on the day of the eclipse. The amplitude of this enhancement appears to be increasing with the progression of the eclipse and maximizing around 16:45 IST at ~225 K. Further, the significant small wave-like features seen around this enhancement which are significant before 16:30 IST and after 17:30 IST are almost minimal during 16:30–17:30 IST.

[10] Figures 4a, 4b, 4c and 4d exhibit the time variation in intensities of the two OH emission (731.6 nm and 740.2 nm) at various distances, for the day of the eclipse and control day. These intensity variations were used for estimating the mesopause temperature. It can be seen that on the day of the eclipse the OH intensities are substantially higher than that on the control day. The OH intensities show an enhancement of ~4 times during the progression of the eclipse. On the otherhand on control day the intensities show a gradual decrease, following typical after noon behavior.

[11] Figures 5a and 5b depict the spatiotemporal variation of the thermospheric O (^{1}D) (630 nm) dayglow intensity on the day of the eclipse and control day respectively. A comparison of these figures clearly indicates that the thermospheric dayglow intensity was significantly higher at off-zenith locations on the day of the eclipse than on the control day around ~15:30–16:00 IST, i.e., ~50–20 m before the first contact on 3 October. The intensity on the control day decreases gradually with time in all directions. However, on the day of the eclipse the thermospheric airglow intensity not only remained significantly high in all directions till 17:30 IST but also it showed an equatorward movement that is relatively more prominent in the northern directions.

[12] The eclipse-induced change in the thermospheric dayglow intensity on 3 October is first seen at the northern most location at around 16:20 IST, i.e., time of first contact. The enhancement in the dayglow intensity begins its equatorward progression, maximizing over the equator at around 16:40 IST. The intensity drop during the course of this progression is ~40%. In the southern direction also, there appears to be an increase in the dayglow intensity that progresses toward equator with time. However, the amount of increase seen in the intensity is significantly smaller than that seen in the northern direction. One interesting observation is that the progression of the enhancement in thermospheric airglow intensity toward equator does not stop over zenith. Instead, as is seen in the Figure 5a it moved almost 100 km south of zenith.

[13] In order to highlight the enhancement in the measured O(^{1}D) dayglow intensity on the day of the eclipse over zenith, the measurements for zenith are compared with the absolute dayglow emission rates, which are estimated using the model formulation of *Zhang and Shepherd* [2004]. The comparison of the measured and estimated intensity on the control day indicates that the comparison is good if the measured intensity is scaled down by a factor of 0.5 (Figure 6). Therefore the intensity variation on the day of

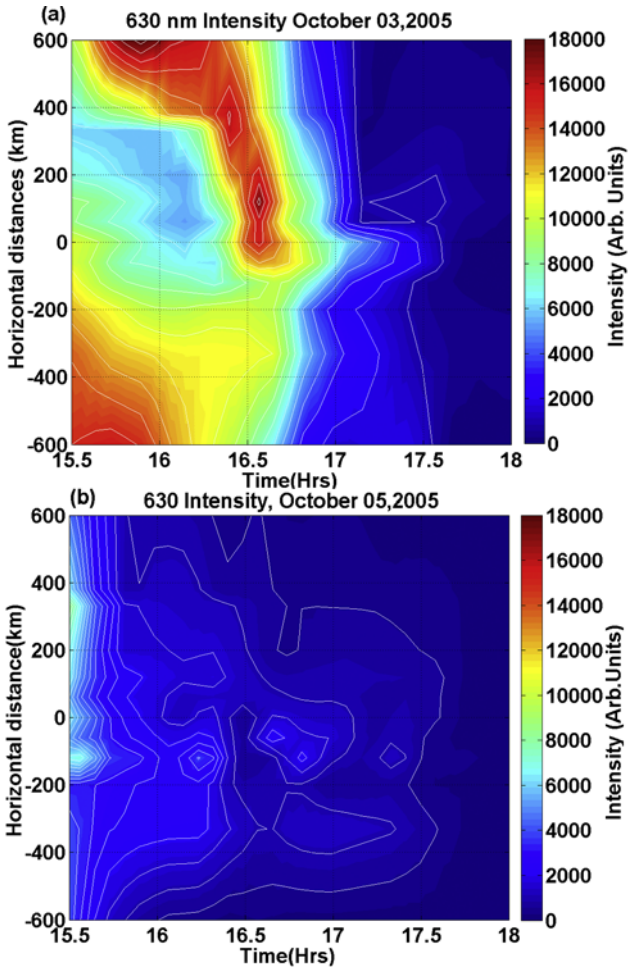

Figure 5. (a and b). Same as Figures 2a and 2b but for the spatiotemporal variation of O(1D) 630 nm intensity (arbitrary units) on 03 and 05 October 2005 respectively.

the eclipse is also obtained using this factor and is depicted in Figure 6 along with the corresponding emission rates estimated using Zhang and Shepherd formulation. It is evident from the figure that on the day of the eclipse the intensity at 15:30 IST is ~1800 R more than the model value. The maximum enhancement seen during the progression of the eclipse is ~8000 R (Rayleigh) which is almost four times higher than the model value. As is known, an enhancement in the ionization density over the O(^{1}D) dayglow altitudes can manifest as an increase in the emission intensity. Therefore to account for this increase in the dayglow intensity, the changes in the ionization density has also been looked into.

[14] Figure 7 shows the variation of VTEC with horizontal distance from zenith on 3 October at around 14:45 IST. On 5 October the satellite pass was at 12:03 IST almost 2 h 45 m earlier than that of the eclipse day. The NIMS satellites didn't pass over Indian longitudes either during the eclipse hours or in that time zone on the control day. Nevertheless, the figure clearly shows that the ionization crest on the day of the eclipse was ~750–1250 km away from zenith in the northern direction and beyond 1250 km in the southern direction. Though the satellite pass was earlier on the control day the anomaly crests appeared to be farther from the dip equator in comparison with the satellite pass corresponding to 14:45 IST on the day of the eclipse. The anomaly crests would have been much farther than this at 14:45 IST on control day and represent a typical behavior of the EIA distribution during afternoon hours. This clearly indicates that on the day of the eclipse the EIA crests are closer than that of the control day.

[15] Figures 8a and 8b shows the variation of GPS measured VTEC with horizontal distance from zenith on 3 October, the eclipse day and 5 October, the control day respectively. It is clear from this figure too that the northern anomaly crest on the day of the eclipse is closer than that on control day, corroborating with Figure 7. Further, it is evident that during the eclipse the TEC over Trivandrum and nearby regions are more (~10 TEC Units) than that on the control day. The TEC enhancement over the dip equator, as seen in this figure, appears to be occurring earlier than the observed dayglow enhancement as seen in Figure 5.

[16] For estimating the prevalent thermospheric meridional wind on the day of the eclipse, the 'two stations' technique formulated by *Krishna Murthy et al.* [1990] is used. The ionosonde measurements during the progression of the eclipse from Sriharikota (SHAR, 13.7°N, 80.2°E, 10°N diplat) and Trivandrum are used for estimating the wind. For reasons elaborated by *Krishna Murthy et al.* [1990], this technique is applicable only in the post evening hours. However, due to the reduced solar insolation during the eclipse, the situation can partially be approximated to evening hours. Therefore the wind estimated here is only indicative of the prevalent wind. Figure 9 depicts the wind during the day of the eclipse which indicates the presence of an equatorward wind between 16:00 and 17:15 IST, turning poleward around 17:00 IST. Further, it must be mentioned that the geomagnetic activity level on the day of the eclipse was moderately high with Kp index being 13, while the control day was relatively quiet (Kp = 7).

[17] Overall, the most striking observations are the almost simultaneous increase in the mesopause temperature over

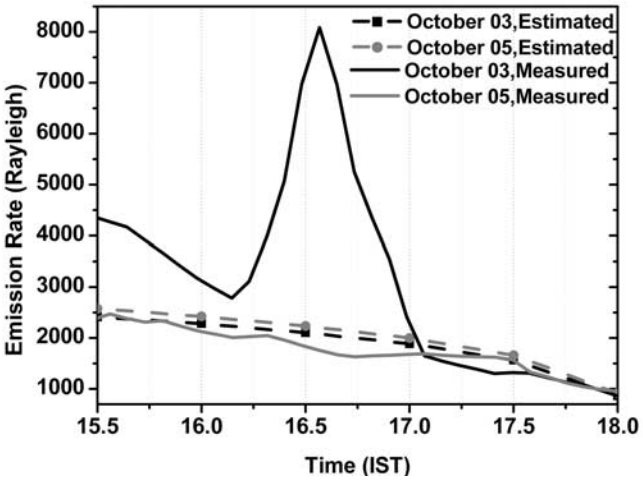

Figure 6. Time variation of the estimated (using the formulations of *Zhang and Shepherd* [2004] and measured thermospheric dayglow emission rates for zenith, during the day of the eclipse and the control day.

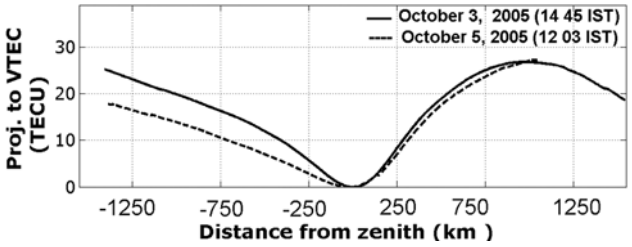

Figure 7. The variation of vertical total electron content (VTEC) with horizontal distance from zenith on 03 October at around 14:45 h (IST) and on 05 October 2005 at 12:03 h (IST).

dip equator and the equatorward progression of thermospheric airglow enhancement.

4. Discussion

[18] The MLTI region over equatorial latitudes is a closely coupled region. During daytime, the wind, which modulates the mesopause energetics and dynamics, also force a global scale dynamo action in the lower ionosphere leading to the generation of electrostatic fields in the zonal and vertical directions. This, in turn leads to the generation of a large scale process called Equatorial Ionization Anomaly (EIA) which significantly controls the latitudinal distribution of low latitude *F* region plasma density. The EIA through its interaction with prevailing dynamics and chemistry leads to the process called Equatorial Temperature and Wind Anomaly (ETWA). In ETWA, collocated with the ionization anomaly crests (trough) thermospheric temperature maxima (minimum) and zonal wind minima (maximum) are formed. As a consequence of these temperature maxima, two meridional circulation cells are established with wind being vertically upward at the crests and downward over the trough, i.e., over the dip equator [*Raghavarao et al.*, 1993 and references therein]. It must be mentioned that the presence of vertically downward wind over the dip equator has been inferred through a number of ground and space based measurements [*Anandarao et al.*, 1978; *Raghavarao et al.*, 1993; *Laakso et al.*, 1995] and the process of ETWA has been modeled [*Maruyama et al.*, 2003]. However, the ETWA associated vertical winds are yet to be modeled satisfactorily.

[19] Under normal conditions, the downward wind over the dip equator is expected to have very small affect in the E-region and below. However, it is conjectured that these winds, as would become clear in the discussion later, can couple the thermosphere-ionosphere region with mesopause and have significant affect in its energetics during special geophysical conditions such as solar eclipse.

[20] In general, the thermal budget of the MLTI is governed by chemistry, dynamics, transport and solar radiation, each one of them responding with their characteristic timescale. For instance, the photochemical lifetime of species (except some species like CO_2) in mesosphere is less than a few tens of seconds. The timescale for ionospheric recombination chemistry in E-region is in minutes while for *F* region it is in hours. In the present case, the eclipse occurred in the evening hours when the solar zenith angle dependence and local time variation is significant for some MLTI parameters, more so for the mesopause and E-region.

[21] In a recent study, *Mlynczack and Solomon* [1993] estimated the mesopause energetics by considering the reaction involving H and O_3 that leads to the vibrationally excited OH, which is radiatively active in the Meinel Band, and is also an important contributor to the chemical heating at the mesopause altitudes. According to their calculations, about 60% of the energy of this reaction is lost as heat while only 40% is released as airglow. The main source of O_3 in the mesopause region is the 3-body recombination of O and O_2. The O is generated through the photolysis of O_2 in the lower thermosphere and brought to mesopause through downward diffusion or mean advection [*Smith*, 2004]. Since the concentration of O_3 is much larger in the night owing to the absence of its photolysis, the resulting chemical heating as mentioned above is also stronger in the night [*Mlynczack and Solomon*, 1993]. Modeling studies have shown that the O_3 mixing ratios in the mesopause region to be high during nighttime [*Smith*, 2004].

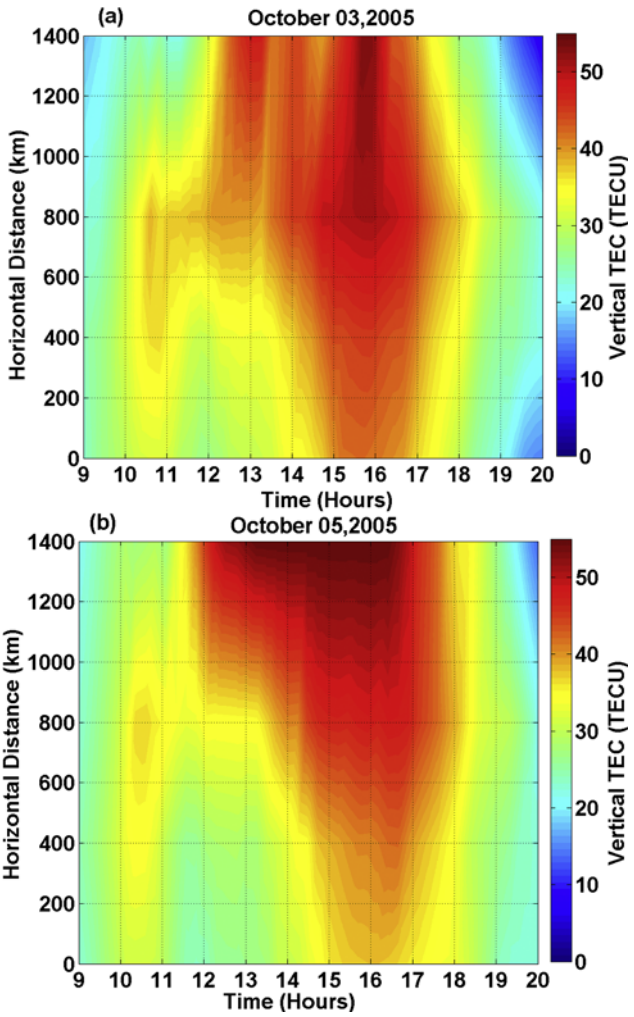

Figure 8. (a and b). The variation of GPS measured vertical total electron content (VTEC) with horizontal distance on Northern side from Trivandrum on 03 October and 05 October 2005 respectively. There are no GPS receivers on the Southern side of Trivandrum.

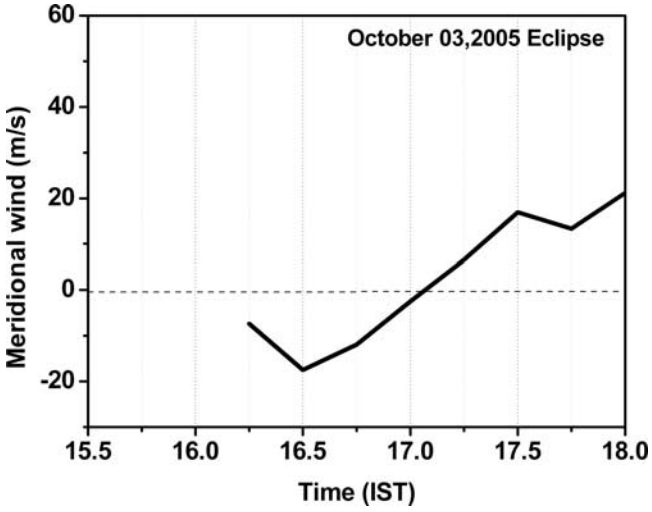

Figure 9. The variation of meridional wind estimated using 'two stations' technique on 03 October. The positive *Y* axis represents the Poleward wind.

[22] Therefore the rise in mesopause temperature around the sunset hours on the control day, i.e., 5 October indicates the gradual increase of O_3 as a part of its diurnal variation. Similarly, on 3 October a part of the enhancement in the mesopause temperature would be due to the increase of O_3 mixing ratios as the eclipse shadow moves over Trivandrum and surrounding regions. In the ionosphere, the density of the E- region would decrease immediately due to the chemistry after the eclipse onset while the *F* region ionization density would not respond immediately. The enhancement in the OH airglow intensities during the eclipse time (Figure 4) clearly supports the role of chemical heating on the mesopause temperature enhancement during the progression of the eclipse. The OH intensities that shows an enrichment of ~4 fold during the eclipse time shows the enhancement in the 3 body reaction, which in turn would manifest as mesopause temperature increase through additional transport of [O] to this region. Apart from photochemistry, during a total solar eclipse the super-sonic movement of the dark spot in the Earth's atmosphere produced by the moon's shadow can lead to the production of internal atmospheric gravity waves [*Chimonas and Hines*, 1970; *Fritts and Alexander*, 2003]. The increase of the mean background temperature on the day of the eclipse may also have a contribution from these waves. However, the temperature enhancement at and around zenith appears to be a consequence of the vertical coupling between the mesopause and thermosphere-ionosphere region. This aspect is discussed later in the following text.

[23] As is known, the main excitation mechanisms for the thermospheric O(^{1}D) 630.0 nm dayglow emission under normal conditions are (i) Photodissociation of O_2 (ii) Photoelectron excitation and (iii) Dissociative recombination. It has been established that the first two mechanisms contribute almost ~70% of the total O(^{1}D) daytime emission [*Zhang and Shepherd* [2004, 2005]; *Thuillier et al.*, 2002]. Further, based on the coordinated dayglow measurements with ionosonde over a low latitude station it has been shown that, although the contribution due to the dissociative recombination is only ~30%, the temporal variability in O(^{1}D) airglow intensity is closely correlated with the electron density within the altitudes for O(^{1}D) 630.0 nm emission i.e., 180–300 km and also the TEC [*Sridharan et al.*, 1992]. It should be borne in mind that the third mechanism, namely dissociative recombination is known to be made up of two parts; one due to the ionization produced in situ by the solar EUV radiation and the other due to the additional ionization electro-dynamically transported from lower latitudes as the EIA develops. The temporal variability of the thermospheric dayglow over a low latitude station has been satisfactorily explained on the basis of these processes [*Sridharan et al.*, 1992]. These various contributors to O(^{1}D) 630.0 nm and O(^{1}S) 557.7 nm dayglow emission have also been modeled [*Culot et al.*, 2004]. A reduction in solar radiation due to eclipse would reduce the solar-induced contributions to dayglow, i.e., photo-dissociation and electron impact by at least the same amount. In this context, the solar obscuration factor of 39% in the present case is expected to decrease the dayglow emission by the same factor, at least. However, contrary to the expectation, the dayglow emission in the present case exhibits a four fold increase, as is shown in Figure 5. This indicates that there must have been an additional source of dayglow emission contributing toward this enhancement.

[24] As mentioned earlier, the variations of the thermospheric airglow over equatorial region are the direct indicator of the changes in the electron density within the altitudes for O(^{1}D) 630.0 nm emission, i.e., 180–300 km and also the TEC [*Sridharan et al.*, 1992]. Therefore the enhanced thermospheric airglow intensity observed around 15:30–16:00 IST on 3 October, in both northern and southern directions appear to be a natural consequence of the anomaly crests being closer. The spatial variation of TEC on this day (Figure 7) shows that the northern and southern anomaly crests are ~750–1250 km and beyond 1250 km away from zenith respectively at 14:45 IST. The extent of asymmetry in the location of the anomaly crests in the northern and the southern hemispheres is usually ascribed to the magnitude and direction of inter-hemispheric wind that, in the present case, appears to be small and from north to south. The satellite pass on the control day was around noon (12:03 IST) when the anomaly is still developing. In other words, the anomaly crests on this day would reach much farther in latitude at a later time viz. ~15:30 IST. This is seen to be true as Figure 8 clearly reveals that the EIA crest is about 1400 km away at a later time on this day. As a consequence, no airglow enhancement is seen at ~15:30 h or afterward on the control day. However, Figure 8 shows that during the time of the eclipse the TEC over zenith and surrounding areas is about 10 units higher on 3 October than the control day. This additional ionization would contribute significantly toward the enhancement of the thermospheric dayglow during the eclipse period.

[25] In this context, the enhancement in the zenithal thermospheric dayglow by ~1800 R at 15:30 IST on the day of the eclipse (Figure 6) appears to be a natural consequence of the increased electron density due to the closer EIA crests. This is further vindicated by the TEC enhancement of ~10 units over zenith at 15:30 IST (Figure 8). In this context, the TEC enhancement observed during the progression of the eclipse is not enough to explain the airglow

enhancement of ~6000 R, i.e., from 2000 to 8000 R at 16:40 IST which is about three times higher than the model value. As explained earlier, if the enhancement in the airglow during the progression of the eclipse is primarily due to the ionization through the dissociative recombination reactions, then in order to explain the observed ~6000 R enhancement in dayglow, the electron density also should increase at least 4 folds and the TEC accordingly. Though an enhancement (~3 TEC w. r. t. the control day) is seen in the TEC over zenith at 16:40 IST, it is small and obviously cannot completely account for the observed dayglow enhancement. Therefore there must be some other processes operating and contributing toward this large enhancement in dayglow on the day of the eclipse.

[26] One such competing effect that could cause variation in the thermospheric emission, at times without inducing significant changes in the TEC, is the change in neutral composition involving the main species like O and N_2 [*Pallamraju et al.*, 2004]. Some of the modeling studies clearly brings out the sensitivity and complexity of the dayglow emission rates to changes in various neutral species. *Melendez-Alvira et al.* [1995] and *Witasse et al.* [1999] respectively presented the modeled sensitivity of 630.0 nm twilight airglow and dayglow to [O_2], [N_2] and [O]. They showed that an increase in O density by a factor of two increases the peak volume emission rate by around 20% through the photoelectron impact mechanism [*Witasse et al.*, 1999]. Similarly, doubling [O_2] can increase the total O(1D) production by at least 60% through photo dissociation and dissociative recombination mechanisms [*Melendez-Alvira et al.*, 1995]. Decrease in the N_2 density by a factor of two increases the red line volume emission rate due to a reduction in quenching by about 15% [*Solomon and Abreu*, 1989; *Melendez-Alvira et al.*, 1995]. In fact *Pallamraju et al.* [2004] showed that a change in O density alone was significant and responsible for the observed O(1D) 630.0 nm dayglow enhancement during a geomagnetic storm. In this context, a part of the overall dayglow enhancement seen on the day of the eclipse could be attributed also to the changes in the neutral density, e.g., density of O, as this day was also geomagnetically moderately disturbed. Nevertheless, in the absence of simultaneous observations of the altitude distribution of the neutral composition, it is difficult to indicate how prominent this factor is vis-a-vis the observed changes in the dayglow emission in the present case.

[27] In a modeling study using the Coupled Thermosphere-Ionosphere-Plasmasphere Model (CTIP), which investigated the in situ-generated changes in the ionosphere and thermosphere during a solar eclipse, it has been shown that not only the ionospheric density but the thermospheric temperature and wind also exhibit significant changes over a wide range of latitudes and longitudes. This study showed that these changes in temperature and wind occur over large latitude (±20°), longitude (±70°) region around the totality with a time lag of about 30 m after the passage of the shadow [*Müller-Wodarg et al.*, 1998, and references therein]. The temperature was shown to decrease overall while the wind especially the meridional wind was shown to change direction for locations north and south of the eclipse totality, with a net convergence over the region of the eclipsed thermosphere.

[28] As a consequence, one would expect the prevalent poleward meridional wind over the low latitude region to decelerate and eventually turn equatorward as the eclipse progresses. It is to be noted that, on a normal day the meridional wind at *F* region heights over these latitudes is poleward in the noon which gradually turns equatorward in the evening hours as the solar insolation slowly decreases over these latitudes [*Wu et al.*, 1994]. Therefore the equatorward wind would cause the ions to move up in altitude and closer to the dip equator. The 10 TEC unit enhancements over and around the dip equator on the day of the eclipse is proposed to be due to the equatorward neutral wind and its effect on the EIA crest. In fact, the presence of the equatorward wind was clearly observed during the progression of the eclipse (Figure 9), vindicating the above aspect. The ionization crest movement toward the equator during a solar eclipse has been seen earlier also [*Huang et al.*, 1999].

[29] However, it must be mentioned that owing to the magnetic field configuration over low latitudes, the additional ionization that is dragged equatorward during the eclipse would first enhance the ionization density in the upper *F* region (where TEC measurements are more sensitive) before registering an effect on the lower F-layer (the altitude region to which OI 630.0 nm dayglow is most sensitive). This would manifest as a time delay between the enhancement seen in the TEC and the dayglow emission intensity. The TEC enhancement would appear earlier than the increase in the dayglow emission. Figure 8 clearly reveals that the TEC enhancement occurs earlier than the corresponding dayglow increase during eclipse. In a study elsewhere, concerning the storm time variability of the 630.0 nm dayglow intensity vis-à-vis the EIA also shows a time difference in the TEC variability and the dayglow variability [*Pallamraju et al.*, 2004].

[30] Since on 3 October, though small there is an inter-hemispheric flow from northern to southern hemisphere; it is capable of pushing ionization across the dip equator. The equatorward movement of ionization seen up to 100 km southward of zenith, as presented here, is attributed to the inter-hemispheric wind. On the day of the eclipse, another manifestation of the enhancement in the ionization density at a given height would be that the ETWA related temperature crests would also get strengthened due to enhanced ion-drag. As a consequence, the meridional wind circulations cells with downward wind over the dip equator would extend to even lower altitudes. This vertically downward wind in a narrow region over the dip equator can then force more O into the mesopause region through enhanced downward diffusion, thereby increasing the chemical heating therein. The additional enhancement in the mesopause temperature in and around zenith as seen in the present case is attributed to this chemical heating. The airglow brightness observed in the OH intensities (Figure 4) during the progression of the eclipse support this argument by demonstrating the need for additional [O] for enhancing the three body reaction and thereby the chemical heating. Further as mentioned earlier, the geomagnetic activity on the day of the eclipse is higher than the control day. This means that there could also be a storm-induced change in the neutral composition at various altitudes in MLTI over the equator. Even in that case, the storm-induced changes in

the mesopause region, if any, are yet to be properly comprehended. Nonetheless, it must be mentioned that there has been no modeling study, which can either satisfactorily generate the altitude profile of the vertical wind associated with ETWA or predict the composition changes in the MLTI region over low latitudes during varying geophysical conditions. Therefore the proposed coupling mechanism at present is a conjecture. Nevertheless, this study highlights the possible vertical coupling of MLTI region over the dip equatorial region, which can become important during transient events like a solar eclipse.

5. Conclusion

[31] Two distinct phenomena have been observed during a solar eclipse event in the MLTI region over equatorial latitudes. The first one is associated with mesopause temperature enhancement and the second one is enhanced thermospheric airglow intensity and its equatorward movement. These observations emphatically show that the MLTI region over the equatorial latitudes respond to the eclipse induced solar forcing. The simultaneity of mesopause temperature change with thermospheric airglow intensity modulations indicate them to be caused by the eclipse induced changes. The present observations suggest that the enhancement in the thermospheric airglow intensity and its equatorward movement is due to the variations in neutral wind, ionization and neutral density, which are also supported by earlier modeling/experimental studies. The mesopause temperature enhancement is attributed to the exothermic mesopause chemistry involving Ozone (O_3). The enhancement in a narrow region around the magnetic equator has been conjectured to be associated with ETWA related vertical wind.

[32] **Acknowledgments.** This work was supported by Department of Space, Government of India. One of the authors C.Vineeth gratefully acknowledges the financial assistance provided by the Indian Space Research Organization through the research fellowship. The authors acknowledge Fred Espanak of NASA/GSFC for Figure 1.

[33] Amitava Bhattacharjee thanks the reviewers for their assistance in evaluating this paper.

References

Altadill, D., J. G. Sole, and E. M. Apostolov (2001), Vertical structure of a gravity wave like oscillation in the ionosphere generated by the solar eclipse of 11 August 1999, *J. Geophys. Res.*, *106*, 21,419–24,428.

Anandarao, B. G., R. Raghavarao, J. N. Desai, and G. Harendel (1978), Vertical winds and turbulence at 93 km over Thumba, *J. Atmos. Terr. Phys.*, *40*, 157–163.

Balan, N., B. V. Krishnamoorthy, C. R. Raghava, P. B. Rao, and K. S. V. Subbarao (1982), Ionospheric disturbances during the total solar eclipse on 16 February 1980, *Proc. Indian Natl. Sci. Acad.*, *48*, 406–415.

Birch, M. J., J. K. Hargreaves, and G. J. Bailey (2002), On the use of an effective ionospheric height in electron content measurement by GPS reception, *Radio Sci.*, *37*(1), 1015, doi:10.1029/2000RS002601.

Chimonas, G., and C. O. Hines (1970), Atmospheric gravity waves induced by a solar eclipse, *J. Geophys. Res.*, *75*, 875–880.

Culot, F., C. Lathuillere, J. Lilensten, and O. Witasse (2004), The OI 630.0 and 557.7 nm dayglow measured by WINDII and modeled by TRANSCAR, *Ann. Geophys.*, *22*, 1–14.

Evans, J. V. (1965), On the behaviour of foF2 during solar eclipse, *J. Geophys. Res.*, *20*, 733–738.

Farges, T., J. C. Jodogne, R. Bamford, Y. Le Roux, F. Gauthier, P. M. Vila, D. Altadill, J. G. Sole, and G. Miro (2001), Disturbance of the western European ionosphere during the total solar eclipse of 11 August 1999 measured by a wide ionosonde and radar network, *J. Atmos. Terr. Phys.*, *63*, 915–924.

Fritts, D. C., and M. J. Alexander (2003), Gravity wave dynamics and effects in the middle atmosphere, *Rev. Geophys.*, *41*(1), 1003, doi:10.1029/2001RG000106.

Ho, C. M., A. J. Mannucci, and U. J. Lindqwister (1996), Global ionospheric perturbations monitored by the worldwide GPS network, *Geophys. Res. Lett.*, 3219–3222.

Huang, C. R., C. R. Liu, K. C. Yeh, K. H. Liu, W. H. Tsai, H. C. Yeh, and J. Y. Liu (1999), A study of tomographically reconstructed ionospheric images during a solar eclipse, *J. Geophys. Res.*, *104*, 79–94.

Kane, J. A. (1966), D region electron density measurements during the solar eclipse of May 20 1966, in *Solar eclipses and the Ionosphere*, Plenum Press, New York, 199.

Krassovsky, V. I. (1972), Infrasonic variations of OH emission in the upper atmosphere, *Ann. Geophys.*, *28*, 739–743.

Krishna Murthy, B. V., S. S. Hari, and V. V. Somayajulu (1990), Nighttime equatorial thermospheric meridional winds from ionospheric h'F data, *J. Geophys. Res.*, *95*, 4307–4310.

Laakso, H., T. L. Aggson, F. A. Herraro, R. F. Pfaff, and W. B. Hanson (1995), Vertical neutral wind in the equatorial F-region deduced from electric field and ion density measurements, *J. Atmos. Terr. Physics*, *57*, 645–651.

Ledig, P. G., M. W. Jones, A. A. Giesecke, and E. J. Chernosky (1946), Effects on the ionosphere at Huancayo, Peru, of solar eclipse, *J. Geophys. Res.*, *51*, 411–418.

Macpherson, B., S. A. Gonzales, M. P. Sulzer, G. J. Bailey, F. Djuth, and R. Rodriguez (2000), Measurements of the topside ionosphere over Arecibo during the total solar eclipse of 26 February 1998, *J. Geophys. Res.*, *10*, 23,055–23,067.

Maruyama, N., S. Watanabe, and T. J. Fuller-Rowell (2003), Dynamic and energetic coupling in the equatorial ionosphere and thermosphere, *J. Geophys. Res.*, *108*(A11), 1396, doi:10.1029/2002JA009599.

Melendez-Alvira, D. J., D. G. Torr, P. G. Richards, W. R. Swift, M. R. Torr, T. Baldridge, and H. Rassoul (1995), Sensitivity of the 6300° A twilight airglow to neutral composition, *J. Geophys. Res.*, *100*, 7839–7853.

Meriwether, J. W. (1985), Ground-based measurements of mesospheric temperatures by optical means, in *Middle atmosphere program handbook for MAP*, edited by R. Vincent, 13, pp 19–40.

Mlynczack, M. G., and S. Solomon (1993), A detailed evaluation of the heating efficiency in the middle atmosphere, *J. Geophys. Res.*, *98*, 10,517–10,541.

Müller-Wodarg, I. C. F., and A. D. Aylward, et al. (1998), Effects of a mid latitude solar eclipse on the thermosphere and ionosphere-A modeling study, *Geophys. Res. Lett.*, *25*, 3787–3790.

Pallamraju, D., S. Chakrabarti, and C. E. Valladares (2004), Magnetic storm-induced enhancement in neutral composition at low latitudes as inferred by O(1D) dayglow measurements from Chile, *Ann. Geophys.*, *22*, 3241–3250.

Pant, T. K., D. Tiwari, S. Sridharan, R. Sridharan, S. Gurubaran, K. S. V. Subbarao, and R. Sekar (2004), Evidence for direct solar control of the mesopause dynamics through dayglow and radar measurements, *Ann. Geophys.*, *22*, 3299–3303.

Raghavarao, R., W. R. Hoegy, N. W. Spencer, and L. Wharton (1993), Neutral temperature anomaly in the equatorial thermosphere-A source of vertical wind, *Geophys. Res. Lett.*, *20*, 1023–1025.

Randhawa, J. S. (1974), Partial solar eclipse effects on temperature and wind in an equatorial atmosphere, *J. Geophys. Res.*, *79*, 5052–5054.

Sastri, J. H., R. Sridharan, and T. K. Pant (2003), Equatorial ionosphere-thermosphere system during geomagnetic storms, *Geophys. Monogr.*, *142*.

Smith, A. K. (2004), Physics and chemistry of the mesopause region, *J. Atmos. Sol. Terr. Phys.*, *66*, 839–857.

Solomon, S. C., and V. Abreu (1989), The 630 nm dayglow, *J. Geophys. Res.*, *94*, 6817–6824.

Sridharan, R., S. A. Haider, S. Gurubaran, R. Sekar, and R. Narayanan (1992), OI 630.0 nm dayglow in the region of equatorial ionization anomaly: Temporal variability and its causative mechanism, *J. Geophys. Res.*, *97*, 13,715–13,721.

Sridharan, R., D. Pallam Raju, and R. Raghavarao (1994), Precursor to equatorial spread-F in OI 630.0 nm dayglow, *Geophys. Res. Lett.*, *21*, 2797–2800.

Sridharan, R., C. V. Devasia, N. Jyoti, D. Tiwari, K. S. Viswanathan, and K. S. V. Subbarao (2002), Effects of solar eclipse on the electrodynamical processes of the equatorial ionosphere: a case study during 11 August 1999 dusk time total solar eclipse over India, *Ann. Geophys.*, *20*, 1977–1985.

Takahashi, H., P. Batista, R. A. Buriti, D. Gobbi, T. Nakamura, T. Tsuda, and S. Fukao (1998), Simultaneous measurements of airglow OH emissions and meteor wind by a scanning photometer and MU radar, *J. Atmos. Sol. Terr. Phys.*, *60*, 1649–1668.

Taylor, M. J., W. R. Pendleton Jr., H. L. Liu, C. Y. She, L. Gardner, R. G. Roble, and V. Vasoli (2001), Large amplitude perturbations in meso-

spheric OH Meinel and 87-km Na lidar temperatures around the autumnal equinox, *Geophys. Res. Lett.*, *28*, 1899–1902.

Thuillier, G., R. H. Wiens, G. G. Shepherd, and R. G. Roble (2002), Photochemistry and dynamics in thermospheric intertropical arcs measured by the WIND Imaging Interferometer on board UARS: A comparison with TIE-GCM simulations, *J. Atmos. Sol. Terr. Phys.*, *64*, 405–415.

Vineeth, C., T. K. Pant, M. Antonita, G. Ramkumar, C. V. Devasia, and R. Sridharan (2005), A comparative study of daytime mesopause temperatures obtained using unique ground-based optical and Meteor wind radar techniques over the magnetic equator, *Geophys. Res. Lett.*, *32*, L19101, doi:10.1029/2005GL023728.

Witasse, O., J. Lilensten, C. Lathuillere, and P. L. Blelly (1999), Modelling the OI630.0 and 557.7 nm thermospheric dayglow during EISCAT-WINDII coordinated measurements, *J. Geophys. Res.*, *104*, 24,639–24,655.

Wu, Q., T. L. Killeen, and N. W. Spencer (1994), Dynamics explorer observations of equatorial thermospheric winds and temperatures: local time and longitudinal dependencies, *J. Geophys. Res.*, *99*, 6277–6288.

Zhang, S. P., and G. G. Shepherd (2004), Solar influence on the O (1D) dayglow emission rate: Global-scale measurements by WINDII on UARS, *Geophys. Res. Lett.*, L07804, *31*, doi:10.1029/2004GL019447.

Zhang, S. P., and G. G. Shepherd (2005), On the response of the atomic oxygen red line emission rates to the Sun's energy input: an empirical model deduced from WINDII/UARS global measurements, *Proc SPIE Vol. 5979, Paper 597912*.

S. Alex, Indian Institute of Geomagnetism, Navi Mumbai, India.

C. V. Devasia, K. Kishore Kumar, T. K. Pant, S. Ravindran, R. Sridharan, S. V. Thampi, and C. Vineeth, Space Physics Laboratory, Vikram Sarabhai Space Centre, Trivandrum, India. (tarun_kumar@vssc.gov.in)